^{1}H NMR Spectroscopic Study of Paramagnetic Lanthanide(III) Texaphyrins. Effect of Axial Ligation

Jerzy Lisowski, Jonathan L. Sessler,* Vincent Lynch, and Tarak D. Mody†

Contribution from the Department of Chemistry and Biochemistry, University of Texas at Austin, Austin, Texas 78712

Received September 26, 1994⊗

Abstract: Paramagnetic Ce(III), Pr(III), Nd(III), Sm(III), Eu(III), Tb(III), Dy(III), Ho(III), Er(III), Tm(III), and Yb(III) texaphyrins were studied in solution using ^{1}H NMR spectroscopic techniques. Key spectroscopic features for the dinitrate complexes **LnTx(NO$_3$)$_2$** were assigned on the basis of 1D NOE, COSY, and ROESY experiments as well as line width and isotropic shift analysis. The observed isotropic shifts can be fit to theoretical models, assuming dipolar contributions are dominant for all but the imino protons. The resulting calculated values are consistent with highly rhombic magnetic susceptibility tensors for those paramagnetic lanthanide texaphyrins in which one of the molecular magnetic axes is roughly perpendicular to the macrocycle plane. For the dinitrate complexes, a change in the magnetic anisotropy was observed between the Ho(III) and Er(III) texaphyrin complexes, a phenomenon that is considered reflective of the changes in metal-centered axial ligation that occur as the lanthanide series is transversed. The derived contact shifts of the imino protons were found to follow well the expected theoretical dependence on $\langle S_z \rangle$. Exchange of both axial nitrate anions for phosphate-type ligands, confirmed by solution phase titration studies, brings about a drastic change in the observed spectral patterns. These changes can be accounted for fully by altering the magnetic susceptibility tensor so as to accommodate what are presumed to be changes in the effective crystal field parameters. Conformation of phosphate coordination in the solid state came from a single crystal X-ray diffraction analysis of the bis(diphenyl phosphate) adduct of Dy(III) texaphyrin. Crystals of $(C_{34}H_{38}N_5O_2)Dy((C_6H_5)_2PO_4)_2{\cdot}0.64(CH_3OH)$ (**DyTx(P1)$_2$**), obtained by diffusion of diphenyl phosphate into methanolic **DyTx(NO$_3$)$_2$** solution, were triclinic, space group $P\bar{1}$, with a = 14.482(3), b = 14.664(3), and c = 15.580(3) Å, α = 69.544(15), β = 65.695(15), and γ = 70.377(15)°, V = 2751.1(11) Å^3, Z = 2, ϱ_{calc} = 1.48 g/cm^{-3}. The structure refined to a final $R(F^2)$ = 0.109 for 644 parameters using 8390 reflections. The Dy(III) ion is seven-coordinate with five donor atoms being provided by the texaphyrin ligand and two by monodentate diphenyl phosphate ions. The Dy(III) ion is only 0.073 Å from the plane through the five nitrogen atoms of the macrocycle. The Dy(III)−O bond lengths are equivalent and average 2.228(5) Å. The Dy−N$_{pyrrole}$ bond lengths average 2.363(3) Å while the Dy−N$_{imine}$ bond lengths average 2.448(4) Å.

Introduction

Texaphyrins (**H·Tx**,[1] Figure 1)[2−10] are aromatic pentadentate ligands that belong to the general class of compounds known as expanded porphyrins.[11] These compounds, while bearing considerable resemblance to the porphyrins, contain a binding cavity that is ca. 20% larger in size. As a result, they form stable 1:1 in-plane, or nearly in-plane, complexes with many cations, including those such as Cd(II), Hg(II), In(III), Ce(III)−Lu(III), that are too large to be accommodated within a central porphyrin core.[12] In the specific case of the trivalent lanthanides, this combination of stability, aromaticity, and structure has made the texaphyrins of interest with regard to a wide variety of potential applications. Currently, for instance, certain gadolinium(III) texaphyrin complexes are being evaluated as possible tissue-selective magnetic resonance imaging[3,9,13] (MRI) contrast agents, while related diamagnetic lutetium derivatives are being studied as photosensitizers for use in the photodynamic eradication of tumors.[5] Recently, europium(III) texaphyrin complexes have also been used to effect the site-specific hydrolysis of RNA.[6] Nonetheless, in spite of the interest these potential applications might engender, structural information in the lanthanide texaphyrin series has been limited to that available

† Current address: Pharmacyclics Incorporated, 995 East Arques Avenue, Sunnyvale, CA 94086.

⊗ Abstract published in *Advance ACS Abstracts,* February 15, 1995.

(1) Abbreviations: **H·Tx**, 4,5,9,24-tetraethyl-16,17-dimethoxy-10,23-dimethyl-13,20,25,26,27-pentaazapentacyclo[20.2.1.1^{3,6}.1^{8,11}.^{14,19}]heptacosa-1,3,5,7,9,11(27),12,14,16,18,20,22(25),23-tridecaene; **H·Tx1**, 4,5-diethyl-10,23-dimethyl-9,24-bis(3-hydroxypropyl)-16,17-bis(3-hydroxypropyl)oxy)-13,20,25,26,27-pentaazapentacyclo[20.2.1.1^{3,6}.1^{8,11}.0^{14,19}]heptacosa-1,3,5,7,9,11(27),12,14,16,18,20,22(25),23-tridecaene; **H·Tx2**, 4,5,9,24-tetraethyl-16,17-bis(3-hydroxypropyl)oxy)-10,23-dimethyl-13,20,25,26,27-pentaazapentacyclo[20.2.1.1^{3,6}.1^{8,11}.0^{14,19}]heptacosa-1,3,5,7,9,11(27),12,14,16,18,20,22(25),23-tridecaene; **P1$^-$**, diphenyl phosphate monoanion; **P2$^-$**, phenylphosphonate monoanion; **P3^{2-}**, phenyl phosphate dianion.

(2) Sessler, J. L.; Hemmi, G.; Mody, T. D.; Murai, T.; Burrel, A.; Young, S. W. *Acc. Chem. Res.* **1994**, *27*, 43.

(3) Sessler, J. L.; Murai, T.; Lynch, V.; Cyr, M. *J. Am. Chem. Soc.* **1988**, *110*, 5586.

(4) Sessler, J. L.; Murai, T.; Hemmi, G. *Inorg. Chem.* **1989**, *28*, 3390.

(5) Harriman, A.; Maiya, B. G.; Murai, T.; Hemmi, G.; Sessler, J. L.; Mallouk, T. E. *J. Chem. Soc., Chem. Commun.* **1989**, 314.

(6) Magda, D.; Miller, R. A.; Sessler, J. L.; Iverson, B. L. *J. Am. Chem. Soc.* **1994**, *116*, 7439.

(7) (a) Maiya, B. G.; Mallouk, T. E.; Hemmi, G.; Sessler, J. L. *Inorg. Chem.* **1990**, *29*, 3738. (b) Sessler, J. L.; Murai, T.; Lynch, V. *Inorg. Chem.* **1989**, *28*, 1333. (c) Kenedy, M. A.; Sessler, J. L.; Murai, T.; Ellis, P. D. *Inorg. Chem.* **1990**, *29*, 1050.

(8) Sessler, J. L.; Mody, T. D.; Ramasamy, R.; Sherry, A. D. *New. J. Chem.* **1992**, *16*, 541.

(9) Sessler, J. L.; Mody, T. D.; Hemii, G. W.; Lynch, V.; Young, S. W.; Miller, R. A. *J. Am. Chem. Soc.* **1993**, *115*, 10368.

(10) Sessler, J. L.; Mody, T. D.; Hemmi, G. W.; Lynch, V. *Inorg. Chem.* **1993**, *32*, 3175.

(11) Sessler, J. L.; Burrell, A. K. *Top. Curr. Chem.* **1991**, *161*, 177.

(12) See, for instance: (a) Schaverien, C. J.; Orpen, A. G. *Inorg. Chem.* **1991**, *30*, 4968. (b) Buchler, J. W.; De Cian, A.; Fischer, J.; Kihn-Botulinski, M.; Paulus, H.; Weiss, R. *J. Am. Chem. Soc.* **1986**, *108*, 3652. (c) Buchler, J. W.; Loffer, J.; Wicholas, M. *Inorg. Chem.* **1992**, *31*, 524 and references cited therein.

(13) Geraldes, C. F. G. C.; Sherry, A. D.; Vallet, P.; Maton, F.; Muller, R. N.; Mody, T. D.; Hemmi, G., submitted for publication.

0002-7863/95/1517-2273$09.00/0

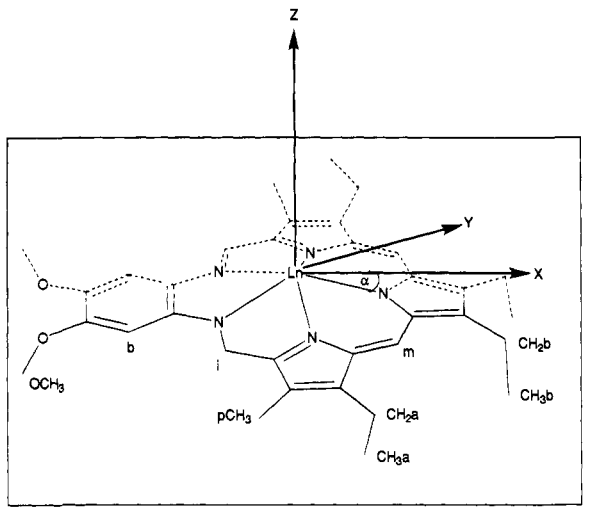

Figure 1. General structure (axial ligands omitted), labeling scheme, and axis system for the dimethoxy tetraethyl dimethyl trivalent lanthanide texaphyrins of this study (abbreviated as **LnTx(NO$_3$)$_2$**. The analogous ligand bearing 3-hydroxypropyl substituents instead of ethyl "a" groups and 3-hydroxypropoxy chains instead of the methoxy substituents is denoted as **Tx1**. The analogous ligand with ethyls "a" in place but bearing 3-hydroxypropoxy chains instead of the methoxy groups is denoted as **Tx2**.

from X-ray diffraction studies of the nitrate complexes. In order to understand better the structure and ligand-based reactivity of these species in solution, we have undertaken a detailed ^{1}H NMR analysis of certain paramagnetic Ln(III) texaphyrins (Ln = lanthanoid = Ce, Pr, Nd, Sm, Eu, Tb, Dy, Ho, Er, Tm, Yb) both in several representative solvents and in the presence of nitrate and phosphate-type counteranions. We have also carried out a single crystal X-ray diffraction analysis of the bis(diphenyl phosphate) adduct of the Dy(III) texaphyrin **[DyTx]$^+$**.

Most lanthanide trivalent ions are paramagnetic and thus induce substantial chemical shifts in the ^{1}H NMR signals of protons located in the vicinity of the metal center.[14] Indeed, the "spreading out" of resonances for organic molecules interacting with paramagnetic complexes has led to the widespread use of paramagnetic lanthanide-containing species as NMR shift reagents.[15,16] On a more fundamental level, the so-called isotropic or additional (i.e., nondiamagnetic) chemical shifts that arise from the interaction of the relevant nuclear and electronic spins can be separated into through-space (i.e., dipolar) and through-bonds (i.e., contact) contributions, respectively. The first of these is dependent on the magnetic anisotropy of the complex in question and the position in space of a given proton, while the second is determined by the nature of the covalent (i.e., bonding) network connecting a given proton with the shift-inducing paramagnetic metal center.

The large magnitude of isotropic shifts and their dependence on bonding and geometry make NMR a much more sensitive tool for probing changes in type of coordination or for assessing subtle conformation changes in paramagnetic lanthanide complexes than it does for the study of their necessarily diamagnetic La(III) and Lu(III) analogs. Nonetheless, while there are numerous reports of paramagnetic NMR effects being used to probe the dynamics of axial ligand exchange in complexes of transition metal ions stabilized by porphyrins and other macrocyclic ligands, this approach has yet to be used extensively in the case of macrocyclic lanthanide complexes. In the particular case of the texaphyrins, such studies are considered to be of fundamental interest in view of the potential biomedical applications being targeted for these systems. For these, it is important to know, for instance, whether the original counteranions in a given administered formulation (e.g., nitrate, acetate, chloride, etc.) will be replaced by other ligands *in vivo* and whether such a putative replacement would have an effect on biodistribution or net whole-body toxicity. Likewise, it is of interest to know whether changes in axial ligation have an effect on either *in vitro* or *in vivo* efficacy. Earlier *in vitro* studies[13] have served to show that the relaxivity of water-soluble gadolinium(III) texaphyrins may be reduced substantially by the addition of phosphates. Phosphate coordination also probably plays a critical role in mediating lanthanide(III)-based RNA hydrolysis, an application for which the texaphyrin-type complexes appear particularly suited.

Experimental Section

The methoxy and hydroxy lanthanide texaphyrins (abbreviated[1] as **LnTx(NO$_3$)$_2$** and **LnTx1(NO$_3$)$_2$**, respectively; see Figure 1) used in this study were prepared as previously described.[10] Diphenyl phosphate monosodium salt (**NaP1**) and phenylphosphonic acid monosodium salt (**NaHP2**) were obtained by reacting the acid forms of these compounds with one stoichiometric equivalent of sodium hydroxide in methanol. The disodium salt of phenyl phosphate (**Na$_2$P3**) was purchased from Aldrich as were the deuterated solvents used in this work.

Complexes of phenyl phosphate dianion, diphenyl phosphate monoanion, or phenylphosphonate monoanion for use in NMR analyses were generally prepared *in situ* by adding known amounts of the phosphate or phosphonate sodium salts to solutions of the chosen Ln(III) texaphyrin nitrate adducts. In the case of the two monoanions, the same solution phase spectra (and hence, presumably, the same complexes) were also obtained when 2,4,6-collidine was added to solutions of the metallotexaphyrin containing the appropriate substituted phosphoric or phosphonic free acids. This was also true if pure, solid samples of the **DyTx(P1)$_2$** were used to prepare the test solutions, provided that a suitable excess of the diphenyl phosphate counteranion was also added.

The pure, solid phosphate adduct of dysprosium texaphyrin **DyTx(P1)$_2$** was prepared by reacting the starting dinitrate texaphyrin with an excess of diphenyl phosphate. The methanol solution of sodium diphenyl phosphate (15 mg, 0.055 mmol) was layered on top of a methanol/dichloromethane solution of dysprosium(III) texaphyrin (9 mg, 0.011 mmol). After 1 week, the resulting green crystalline precipitate was filtered, washed with methanol, and dried (9.5 mg, 0.0077 mmol, 70% yield).

(14) For NMR analyses of paramagnetic complexes see the following: (a) La Mar, G. N., Horrocks, W. DeW., Jr., Holm, R. H., Eds. *NMR of Paramagnetic Molecules*; Academic Press: New York, 1973. (b) Bertini, I.; Luchinat, C. *NMR of Paramagnetic Molecules in Biological Systems*; Benjamin/Cummings: Menlo Park, CA, 1986. (c) Bertini, I.; Turano, P.; Vila, A. J. *Chem. Rev.* **1993**, *93*, 2833.

(15) For reviews of shift reagents and paramagnetic NMR of lanthanide complexes, see the following: (a) Horrocks, W. DeW., Jr., Chapter 12 in ref 14a. (b) Fisher, R. D., Chapter 13 in ref 14a. (c) SIvers, R. E., Ed. *Nuclear Magnetic Resonance Shift Reagents*; Academic Press, Inc.: New York, 1973. (d) Reuben, J.; Elgavish, G. A. In *Handbook on the Physics and Chemistry of Rare Earths*; Gschneider, K. A., Jr., Erying, L., Eds.; North-Holland Publishing Company: Amsterdam, 1979; Chapter 38. (e) Ascenso, J. R.; Xavier, A. V. In *Systematics and the Properties of the Lanthanides*; Shina, S. P., Ed.; D. Reidel Publishing Company; Dordrecht, 1983; Chapter 11. (f) Sherry, A. D.; Geraldes, C. F. G. C. In *Lanthanide Probes in Life, Chemical, and Earth Sciences Theory and Practice*; Bunzli, J.-C. G., Ed.; Elsevier: Amsterdam, 1989; Chapter 4.

(16) There is a vast literature on the use of paramagnetic complexes as shift reagents. For example see: (a) Marinetti, T. D.; Snyder, G. H.; Sykes, B. D. *J. Am. Chem. Soc.* **1975**, *97*, 6562. (b) Horrocks, W. De W., Jr.; Sipe, J. P., III. *Science* **1972**, *177*, 994. (c) Dobson, C. M.; Geraldes, C. F. G. C.; Ratcliffe, G.; Williams, R. J. P. *Eur. J. Biochem.* **1978**, *88*, 259. (d) Geraldes, C. F. G. C.; Williams, R. J. P. *Eur. J. Biochem.* **1978**, *85*, 463. (e) Bassfield, R. L. *J. Am. Chem. Soc.* **1983**, *105*, 4168. (f) Singh, M.; Reynolds, J. J.; Sherry, A. D. *J. Am. Chem. Soc.* **1983**, *105*, 4172. (g) Lee, L.; Sykes, B. D. *Biochemistry* **1983**, *22*, 4266. (h) Babushkina, T. A.; Zolin, V. F.; Koreneva, L. G. *J. Magn. Reson.* **1983**, *52*, 169. (i) Jenkins, B. G.; Lauffer, R. B. *J. Magn. Reson.* **1988**, *80*, 328. (j) Konami, H.; Hatano, M. *Chem. Phys. Lett.* **1989**, *160*, 163. (k) Sink, R. M.; Buster, D. C.; Sherry, A. D. *Inorg. Chem.* **1990**, *29*, 3645. (l) Geraldes, C. F. G. C.; Sherry, D. A.; Kiefer, G. E. *J. Magn. Reson.* **1992**, *97*, 290.

Single crystals of the bis(diphenyl phosphate) adduct of **[DyTx]$^+$**, suitable for X-ray diffraction analysis, were grown on a smaller scale in an analogous way from methanol/methanol-d_4 solutions. Here, the methanol-d_4 was used to generate **DyTx(NO$_3$)$_2$** solutions of higher specific gravity. Diffraction data were collected at −100 °C on a Nicolet P3 diffractometer using graphite-monochromated Mo Kα radiation ($\lambda = 0.71073$ Å). The crystal system is triclinic and the space group is $P\bar{1}$, with $a = 14.482(3)$, $b = 14.664(3)$, and $c = 15.580(3)$ Å, $\alpha = 69.544(15)$, $\beta = 65.695(15)$, and $\gamma = 70.377(15)°$, $V = 2751.1(11)$ Å^3, $Z = 2$, $\varrho = 1.48$ g cm^{-3}, $F(000) = 1257$ for $(C_{34}H_{38}N_5O_2)Dy((C_6H_5)_2PO_4)_2{\cdot}0.64(CH_3OH)$. Data, 8390 unique values, were collected out to a maximum 2θ of 47.5° using the ω-scan technique, with a scan range of 1.2° at a scan rate of 3−6°/min. Data reduction and decay corrections were performed using the SHELXTL-*Plus* software package.[17] The structure was solved by a combination of Patterson and direct methods.[17] The structure refined to a $R_w(F^2) = 0.109$ using 8390 reflections, refining 644 parameters, goodness-of-fit = 1.077. The convention R index based on $F > 4(\sigma(F))$ is equal to 0.0466 for 6619 reflections. Full X-ray experimental details and tables of positional and thermal parameters and geometric factors are given in the supplementary material.

Proton NMR spectra were recorded using Bruker AC-250 and AM-500 spectrometers and General Electric QE-300 and GE GN500 instruments. Observed chemical shifts were referenced to TMS or to easily identifiable solvent signals. Since the solubilities of the studied complexes were found to vary greatly (in a rather irregular fashion) as the lanthanide series was transversed, the relevant sample concentrations necessarily ranged from ca. 0.1 to 10 mM, while the number of scans collected per spectrum was accordingly varied from 100 to 6000. The spectra were measured in mixtures of MeOH-d_4 and $CHCl_3$-d or in pure MeOH-d_4, with the former solvent generally affording a higher concentration of dissolved complex. Spectra of representative hydroxylated Ln texaphyrins **LnTx1(NO$_3$)$_2$** were also recorded in D_2O.

Two dimensional (2D) experiments were carried out at 500 MHz. COSY spectra were acquired using 512 data points in F_1 and 1024 data points in F_2. The data were processed by using a sine bell window and zero filling to 1K data points in both dimensions. NOESY were recorded using a 256 × 2024 data matrix zero filled to 2K × 2K with the same window function being applied. The phase sensitive (TPPI) ROESY (50 ms spin lock) of the Nd texaphyrin complex was measured at 323 K in order to have better line resolution and shorter T_1s. Here, a 512 × 1024 data matrix was zero filled to 1K × 1K and a square sine bell window function was used. T_1 values were measured on the 500 MHz GE GN500 spectrometer using standard inversion−recovery methods. Software provided by the manufacturer was used to fit the relaxation data. Values of T_2s were estimated from line widths.

Isotropic shifts were calculated using relevant lanthanum(III) or lutetium(III) texaphyrins as diamagnetic references (the assignments reported in ref 9 were checked using NOESY). The resulting isotropic shift values were then fit to eq 3 (cf. Results and Discussion) using a nonlinear least-squares fit of the D_1 and D_2 parameters as well as the rotation angle α to about the x axis of χ tensor as defined in Figure 1. The calculation was accomplished by minimizing the agreement factor (eq 1):

$$R = [\sum(\delta^{obs}_{iso} - \delta^{calc}_{dip})^2/\sum(\delta^{obs}_{iso})^2]^{0.5} \quad (1)$$

Here, the attainment of the global minimum was tested by using different starting parameters. Sets of equivalent minima were also obtained even after rotation of the axis system by 90°. The relevant starting geometric factors for each proton were derived from the coordinates of the X-ray diffraction structures of the disordered 9-coordinate gadolinium texaphyrin complex **GdTx(NO$_3$)$_2$**.[10] For the Ce(III), Pr(III), Nd(III), and Eu(III) **LnTx(NO$_3$)$_2$** complexes (the latter presumably being isostructural with that for Gd(III)[10]), the "larger" (i.e., higher coordinate) **LaTx(NO$_3$)$_2$** structure was also used as starting point; this was found to give very similar results. For the diphenyl phosphate complexes, the relevant geometric factors were derived from both the **DyTx(P1)$_2$** structure and the disordered 9-coordinate **GdTx(NO$_3$)$_2$** structure. The positions of the protons on the methyl, ethyl, and methoxy substituents were averaged, assuming free rotation of these substituents. In all cases, the starting axis system of the χ tensor used in calculations was defined by an x axis defined by the Ln(III) center and the nitrogen of the central tripyrrane pyrrole and an xz plane defined by the same pyrrolic nitrogen, the Ln(III) ion in question, and a point midway between the two imino nitrogens (Figure 1). In some cases, a modified axis labeling procedure was also used. Here, the z axis was exchanged with the y axis, and the ensuing rotation performed in the xy plane, with equivalent results being obtained (see below).

(17) Sheldrick, G. M. SHELXTL-*Plus* (Version 4.11), 1991. Siemens X-ray Analytical Instruments, Inc., Madison, WI.

Results and Discussion

Symmetry Considerations. Representative ^{1}H NMR spectra, recorded at 296 K in methanol-d_4 or methanol-d_4/chloroform-d_1, for the paramagnetic lanthanide texaphyrins of general formula [Ln(texaphyrin)](NO$_3$)$_2$·n(CH$_3$OH) (**LnTx(NO$_3$)$_2$**), where **Ln** = Ce(III), Pr(III), Nd(III), Eu(III), Sm(III), Tb(III), Dy(III), Ho(III), Er(III), Tm(III), and Yb(III), are provided in the top frames of Figures 2 and 3 and in supplementary Figures 7 and 8. While a wide range of chemical shift values, ranging from 107 ppm for the Dy(III) complex to −75 ppm for the Tm(III) derivative (cf., also Table 1), and some diversity in terms of signal resolution are observed, in general these spectra are made simple by the presence of a clear 9-line peak pattern. For the possibly diastereotopic methylene protons CH$_2$a and CH$_2$b (see below for details of peak assignments), only one peak is observed at 296 K (corresponding to an effective C_{2v} symmetry). However, variable temperature measurements carried out using the Nd(III) and Tb(III) complexes **NdTx(NO$_3$)$_2$** and **TbTx(NO$_3$)$_2$** show that at lowered temperatures (below 273 K) these same signals are split into two peaks each, indicating that the system is of C_s symmetry. This behavior can be explained by fast rotation of the ethyl substituents at higher temperatures in structures such as **I** and **II** (Scheme 1) that are otherwise of nominal C_s symmetry. Alternatively, in analogy to what is observed in the case of iron porphyrins,[18] the apparent C_{2v} symmetry observed at high temperature could result from a ligand exchange and metal flip-flop averaging of out-of-plane structures, of types **I** and **II** (Scheme 1), rather than from the specific presence in solution of more symmetric species such as those represented by structures **III** and **IV** in Scheme 1.[19]

Spectral Assignments. In the case of the neodymium complex **NdTx(NO$_3$)$_2$**, the observed T_1 relaxation times were long enough to allow both 2D and NOE measurements to be made, thus allowing unequivocal spectral assignment. From integrations of the ^{1}H NMR spectrum of the Nd(III) complex **NdTx(NO$_3$)$_2$**, signals corresponding to the various methyl and methylene protons could be differentiated from one another and

(18) (a) La Mar, G. M.; Walker, F. A. In *The Porphyrins*; Dolphin, D., Ed.; Academic Press: New York, 1979; Vol. IV, Chapter 2, pp 142−146. (b) La Mar, G. N. *J. Am. Chem. Soc.* **1973**, *95*, 1662.

(19) While the available data do not permit a rigorous distinction between these two limiting mechanistic explanations, some insight can be obtained by reference to the literature. In the case of the aquo adduct of octaethylporphinatothalium(III) hydroxide, for instance, the activation energy for ethyl rotation is estimated to be ca. 80 kJ/mol.[20] Likewise, in the case of OEPFeCl, the available data indicate that the barrier for this process must be higher than 70 kJ/mol.[18b] On the other hand, in the case of the Nd(III) and Tb(III) texaphyrin complexes discussed above, temperature-dependent NMR analysis shows that the activation free energies ($\Delta G^{\ddagger}$) associated with the process responsible for signal averaging are far lower ($\Delta G^{\ddagger} = 56 \pm 1$ and 48 ± 1 kJ/mol for these two complexes, respectively). Since the energetic barrier for pyrrole ethyl rotation is expected to be similar in texaphyrins and porphyrins, it is concluded that such rotational processes cannot be responsible for the observed signal averaging at higher temperatures. Rather, it is proposed, flip-flop averaging of out-of-plane structures (i.e., the second mechanism above) play a dominant role. Thus, generalized structures of type **Ia** and/or **IIa** in Scheme 1 (in rapid equilibrium with counterparts, **Ib** and **IIb**), rather than **III** and **IV**, would be expected to represent best the dominant species in solution.

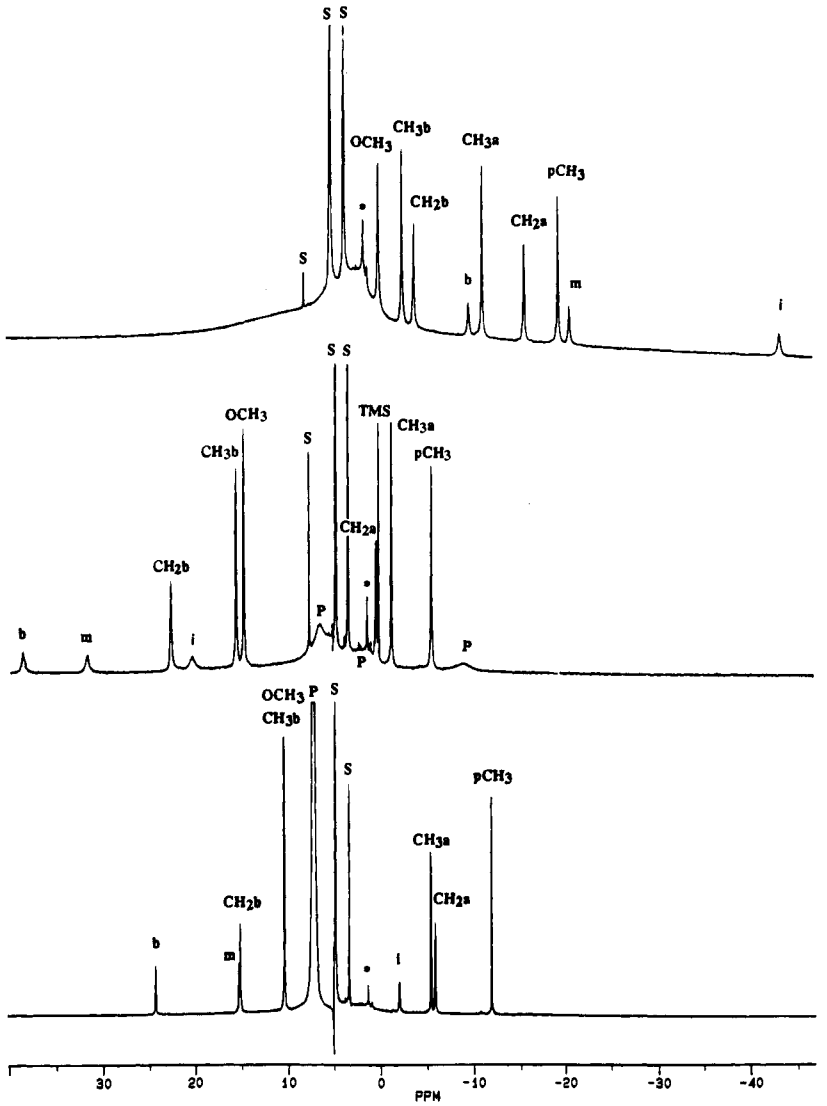

Figure 2. Proton NMR spectra (296 K) of Yb(III) texaphyrin complexes of general structure **YbTx(X)$_2$** recorded using nitrate (top, 2 mM solution in $CDCl_3/CD_3OD$ 2:1 v/v), phenylphosphonate (middle, 3.6 mM solution in $CDCl_3/CD_3OD$ 1:1 v/v, 10 equiv of monosodium phenylphosphonate), and diphenyl phosphate (bottom, 2 mM solution in $CDCl_3/CD_3OD$ 1:1 v/v, 10 equiv of sodium diphenyl phosphate) as the counteranions. P denotes signals arising from the phenyl protons of diphenyl phosphate or phenylphosphonate and S those from solvent and DHO signals; and an asterisk those from impurities.

from the combined set of yet-unassigned signals corresponding to imino, benzo, and meso protons (for labeling, see Figure 1). The methylene and methyl signals of the ethyl substituents could then be combined into pairs on the basis of corresponding crosspeaks in the COSY spectrum (supplementary Figure 9). Once this was done, 1D difference NOE (supplementary Figure 10) and ROESY (Figure 4) spectra were used to make more detailed assignments. An NOE effect, for instance, was seen between the two methylene protons and the two protons giving rise to the signal at 11.25 ppm (Figure 4, shift values refer to 296 K) which, on this basis, were assigned as the meso-like protons of the tripyrrolodimethine portion of the macrocycle. Likewise, the most downfield signal in the ^{1}H NMR spectrum at 29.90 ppm, integrating to 2H, was found to give NOEs to the signal at 8.92 ppm (integrating to 2H) and to a methyl signal at 6.58 ppm (supplementary Figure 10). The signal at 8.92 ppm was also found, in turn, to be cross-correlated to the methyl signal at 4.21 ppm. Thus, on this basis, the pair of signals at 8.92 and 4.21 ppm could be assigned to the benzo and OCH_3 protons and the pair at 29.90 and 6.58 ppm to those of the imino bridge and the pyrrole CH_3 substituents, or vice versa.

NOEs involving ethyl substituents (not shown) confirm the critical COSY pair assignments and the assignment of the signal ascribed to the meso-like protons. In addition, the ethylene methyl protons (signal at 3.59 ppm) were found to be correlated with a methyl signal at 6.58 ppm. On this basis, the connection between the pyrrole methyl groups and the ethyl substituents on the same pyrrole was established. Establishing this connection means that (1) the signals at 6.83 and 3.59 ppm correspond to the CH_2a and CH_3a components of the ethyl substituent "a", (2) the signals at 3.25 and 1.06 ppm correspond to those protons labeled CH_2b and CH_3b, the 6.58 ppm signal to the pyrrole CH_3 subunit, the peak at 29.90 ppm to the imino proton, and (3) the signal at 4.24 ppm belongs to the OCH_3 moiety and the signal at 8.92 ppm may be assigned to the benzo proton.

Exactly the same type of assignments was obtained from the COSY and 1D NOE difference spectra for the praseodymium(III) texaphyrin complex **PrTx(NO$_3$)$_2$**. Also, similar NOEs were observed for the cerium(III) texaphyrin derivative **CeTx(NO$_3$)$_2$**, except that the NOE between the pyrrole methyl and the ethyl "a" group was too weak to be detected.

In the case of Tb(III) and Er(III) complexes **TbTx(NO$_3$)$_2$** and **ErTx(NO$_3$)$_2$**, the relaxation rates were too short to allow

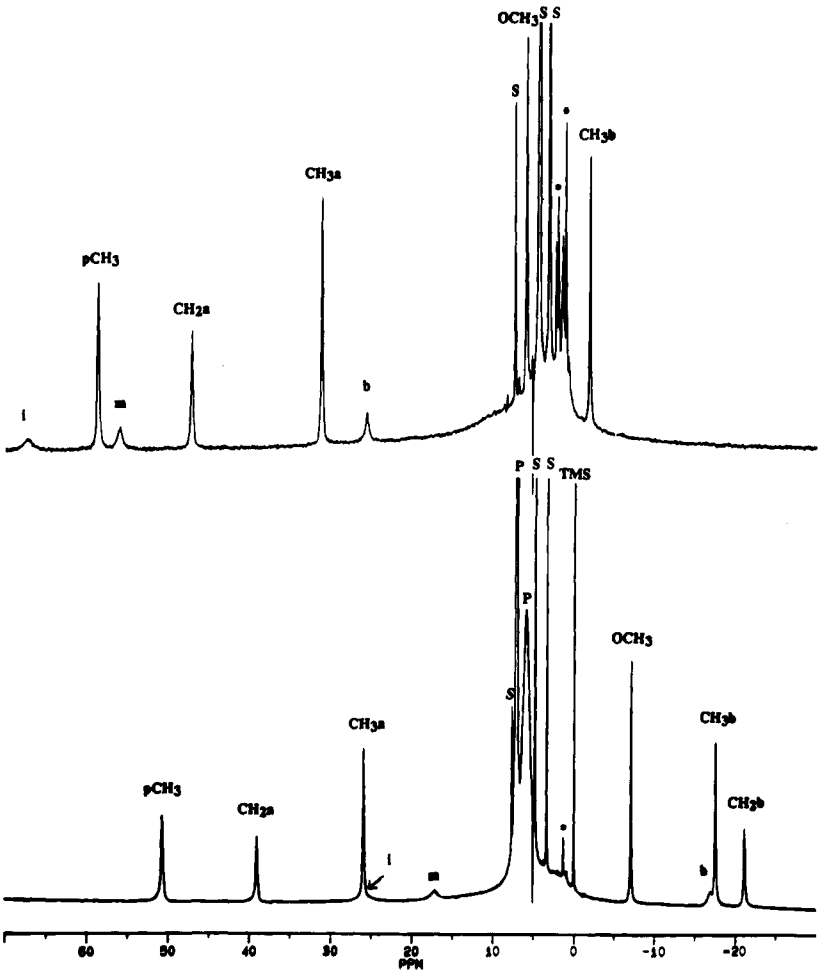

Figure 3. Proton NMR spectra (296 K) of the Ho(III) texaphyrin complexes of general structure $\mathbf{HoTx(X)_2}$ recorded using nitrate (top, 3 mM solution in $CDCl_3/CD_3OD$ 3:2 v/v) and diphenyl phosphate (bottom, 4.3 mM solution in $CDCl_3/CD_3OD$ 1:1 v/v, 10 equiv of sodium diphenyl phosphate) as the counteranions. P denotes signals arising from the phenyl protons of diphenyl phosphate, S those from solvent and DHO, and an asterisk those from impurities.

Table 1. Isotropic Shifts (ppm) of Lanthanide Texaphyrin Nitrate Complexes ($\mathbf{LnTx(NO_3)_2}$)[a]

	Ce[b]	Pr[b]	Nd[b]	Eu[b]	Tb[b]	Dy[b]	Ho[b]	Er[b]	Tm[c]	Yb[b]
imino	6.23	16.90	18.47	−31.20	29.84	96.0	55.60	−64.53	−86.63	−55.83
meso	1.15	2.15	1.67	−1.42	58.00	71.62	46.17	−25.48	−45.01	−30.88
benzo	0.39	0.45	−0.10	−0.09	26.22	23.07	16.37	−8.36	−24.81	−19.72
CH_2a	1.50	3.93	3.36	−3.54	43.74	70.43	43.41	−14.74	−30.61	−19.60
p-CH_3	1.60	4.46	3.57	−3.50	54.75	100.1	55.38	−16.22	−34.00	−7.16
OCH_3	0.26	0.04	−0.07	−0.02	5.11	0.67	1.54	−4.75	−5.54	−4.98
CH_3a	1.10	2.53	2.14	−1.87	29.81	47.48	29.48	−9.67	−20.23	−13.17
CH_2b	0.28	−0.53	−0.22	−0.17	4.71	−6.06	−2.09	−9.40	−10.24	−7.85
CH_3b	0.21	−0.61	−0.39	0.32	1.03	−8.24	−3.47	−5.57	−5.32	−4.55

[a] 296 K. [b] $CDCl_3/CD_3OD$ 1:1 v/v. [c] CD_3OD.

an NOE effect to be detected. Also, it was obvious that for the trivalent Dy, Ho, Tm, and Yb complexes $\mathbf{DyTx(NO_3)_2}$, $\mathbf{HoTx(NO_3)_2}$, $\mathbf{TmTx(NO_3)_2}$, and $\mathbf{YbTx(NO_3)_2}$, NOEs would not be observed due to short T_1 and/or low solubilities. For the Sm(III) texaphyrin $\mathbf{SmTx(NO_3)_2}$ with its very small isotropic shifts and sharp signals, assignments could be made by simple comparison back to the diamagnetic La(III) complex $\mathbf{LaTx(NO_3)_2}$.

For the remaining paramagnetic lanthanide texaphyrins, resonance assignments were made on the basis of signal integrations and line width analyses and the results obtained for the Nd(III), Pr(III), and Ce(III) complexes.

For the paramagnetic complexes the ratios of $T_{1\,dip}^{-1}$ for different positions should be proportional to the ratios of the inverse sixth powers of the relevant metal−proton distances.[21] On the basis of the X-ray structure of the Gd(III) complex $\mathbf{GdTx(NO_3)_2}$, these latter are calculated as being equal to 100:50.99:30.41:10.41:8.60:8.38:5.22:5.16:2.14 for the imino, meso, benzo, pyrrole CH_3, CH_2a, CH_2b, CH_3b, CH_3a, and OCH_3 protons, respectively. In accord with this expected theoretical trend, values of T_1, measured experimentally for the Nd(III) and Tb(III) complexes $\mathbf{NdTx(NO_3)_2}$ and $\mathbf{TbTx(NO_3)_2}$ by the inversion recovery method, gave ratios of 10048.61:29.54:13.20:13.23:14.50:8.03:8.09 and 100:82.46:32.39:16.45:11.54:11.27:8.01:6.25:4.43 for these particular Nd(III) and Tb(III) texaphyrin complexes, respectively.

When the dipolar transverse relaxation is the dominant line-

(20) Abraham, R. J.; Smith, K. M. *Tetrahedron Lett.* **1971**, *36*, 3335.

(21) For a discussion of relaxation processes in paramagnetic systems, see refs 15 and 24f, and references cited therein. See also: Bertini, L.; Capozzi, F.; Luchinat, C.; Nicastro, G.; Xia, Z. *J. Phys. Chem.* **1993**, *97*, 6351.

Scheme 1. Nitrate Dissociation Equilibria for Lanthanide Texaphyrins (Coordinated Solvent Omitted)

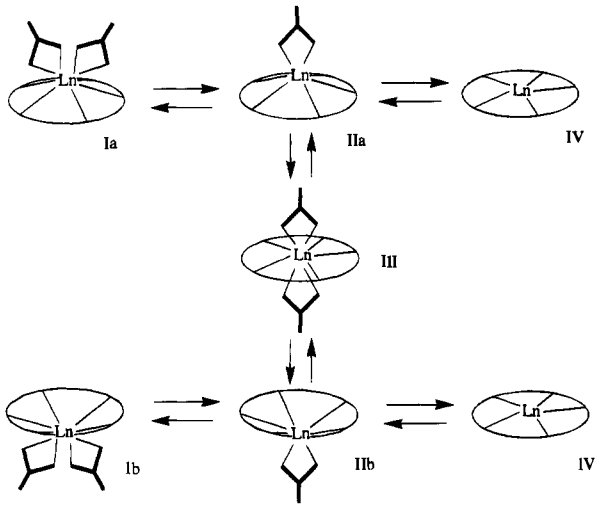

broadening factor, line widths are also expected to exhibit an r^{-6} dependence.[21] Thus, it is clear that signals integrating to two protons for the pyrrole and methoxy methyl substituents. These latter can also be distinguished from the ethyl methyls on this basis. Unfortunately, however, a distinction *between* pairs of methylene and *between* the methyl signals of the two distinct "a" and "b" ethyl substituents cannot be made on this basis because the relevant distances (and relaxation rates) are too similar. This distinction can, however, be made on the basis of similarities in the ratios of the shifts observed for the different positions as the series of trivalent lanthanide texaphyrins is transversed (using the assignments made for the Nd(III), Pr(III), and Ce(III) texaphyrin complexes and assuming dipolar contribution are dominant for these positions throughout the lanthanide series). This is because, for a series of strictly isostructural lanthanide complexes with no contact contribution to the isotropic shift and χ tensor of an axial symmetry (or nonaxial tensor with constant D_1/D_2 ratio along the lanthanide series), a constant ratio of isotropic shifts is expected as a consequence of the invariance of the relevant geometric factors.[15] Thus, for the various other **LnTx(NO$_3$)$_2$** complexes in question, the signals for ethyl "a" are predicted to lie closer to the pyrrole methyl signal than those of ethyl "b".

The dipolar shifts of a given proton within a series of isostructural lanthanide complexes should be proportional to the theoretical Bleaney coefficients C_j.[15,22] Working on this assumption, plots of isotropic shifts vs Bleaney coefficients were made (cf. supplementary material) and used to correlate the observed chemical shifts of the Nd(III), Pr(III), and Ce(III) texaphyrins with those of the other lanthanide texaphyrin complexes. As expected, the relevant plots are not strictly linear since the complexes within the series studied are similar, but not exactly isostructural; crystal structures, for instance, of the congeneric nitrate complexes **LaTx(NO$_3$)$_2$**, **GdTx1(NO$_3$)$_2$**, and **LuTx2(NO$_3$)$_2$** show a reduction in the out-of-plane displacement and a decrease in the net coordination number about the central metal as the lanthanide series is transversed.[10] Also, as will be shown later, the contact contribution is not negligible in all positions and the χ tensor is definitely nonaxial. Nevertheless, for the trivalent Tb, Dy, Ho, Er, Tm, and Yb complexes, this type of plot was useful in assigning the resonances within groups of signals (e.g., meso, imino, and benzo) of the same integration intensity. The assignments obtained in this way are in good agreement with those obtained from line width analysis. Final verification then came as the result of carrying out comparisons between the observed isotropic shifts and those fit on the basis of theory as discussed below; the assignments based on these plots of isotropic shifts vs Bleaney coefficients gave the best internal agreement. In particular, interchanging the assignments of the signals for the ethyl substituents "a" and "b" (i.e., those that might be considered most tenuous) caused a drastic deterioration in the agreement factor R. Thus the given assignments are considered to be secure.

Calculation of Dipolar Shifts. Assessment of Contact Contributions. (1) Fitting Procedures. The isotropic shifts (δ_{iso}) of paramagnetic lanthanide complexes can be considered in terms of contributions from both dipolar (δ_{dip}) and contact (δ_{cont}) terms:

$$\delta_{iso} = \delta_{dip} + \delta_{cont} \tag{2}$$

Generally, the contact contribution quickly diminishes as the number of bonds between a given Ln^{3+} ion and the monitored nucleus increases. Therefore, in making the following analysis we started with the common assumption that the proton shifts of lanthanide complexes are dominated by dipolar contributions, as given by the formula:[23]

$$\delta_{dip} = D_1G_1 + D_2G_2 = D_1\left\langle\frac{1 - 3\cos^2\theta}{r^3}\right\rangle + D_2\left\langle\frac{\sin^2\theta\cos 2\varphi}{r^3}\right\rangle \tag{3}$$

where

$$D_1 = \frac{\bar{\chi} - \chi_{zz}}{2N},\ D_2 = \frac{\chi_{xx} - \chi_{yy}}{2N}$$

In this expression, χ_{xx}, χ_{yy}, and χ_{zz} are the principal components of the magnetic susceptibility tensor and r, θ, and φ are polar coordinates of a given proton.

Many authors have fit the observed isotropic shifts of paramagnetic lanthanide complexes to expressions for dipolar shift.[24] In our case, since the spectra exhibit features associated with C_s symmetry, we assumed that two of the principal axes of the molecular susceptibility tensor should lie within the symmetry plane of the complex. As a consequence, we considered that only three (rather than five) parameters, namely the anisotropy factors D_1 and D_2 and the orientation of the magnetic axes in the symmetry plane (given, e.g., by the rotation angle α as defined in Figure 1) would need to be varied such that the δ_{dip} values of eq 3 would provide the best fit to the observed isotropic shifts.

The above reliance on three parameters, attractive as it is, nonetheless requires the use of one more parameter than would be needed under conditions of assumed axial symmetry (e.g., $D_1 \neq 0$, $D_2 = 0$). Thus, we first checked whether our

(22) (a) Bleaney, B. *J. Magn. Reson.* **1972**, *8*, 91. (b) Bleaney, B.; Dobson, C. M.; Levine, B. A.; Martin, R. B.; Williams, R. J. P.; Xavier, A. V. *J. Chem. Soc., Chem. Commun.* **1972**, 791.

(23) (a) McConnell, H. M.; Robertson, R. E. *J. Chem. Phys.* **1958**, *29*, 1361. (b) Kurland, R. J.; McGarvey, B. R. *J. Magn. Reson.* **1970**, *2*, 286.

(24) See for example: (a) Barry, C. D.; North, A. C. T.; Glasel, J. A.; Williams, R. J. P.; Xavier, A. V. *Nature* **1971**, *232*, 236. (b) Willcot, M. R., III; Lenkinski, R. E.; Davis, E. D. *J. Am. Chem. Soc.* **1972**, *94*, 1744. (c) Cramer, R. E.; Dubois, R.; Seff, K. *J. Am. Chem. Soc.* **1974**, *96*, 4125. (d) Agresti, D. G.; Lenkinski, R. E.; Glickson, J. D. *Biochem. Biophys. Res. Commun.* **1977**, *76*, 711. (e) Peters, J. A.; Nieuwenhuizen, M. S. *J. Magn. Reson.* **1985**, *65*, 417. (f) Kemple, M. D.; Ray, B. D.; Lipkowitz, K. B.; Prendergast, F. G.; Rao, B. D. N. *J. Am. Chem. Soc.* **1988**, *110*, 8275. (g) Aime, S.; Botta, M.; Ermondi, G. *Inorg. Chem.* **1992**, *31*, 4291. Capozzi, F.; Cremonini, M. A.; Luchinat, C.; Sola, M. *Magn. Reson.* **1993**, *31*, S118.

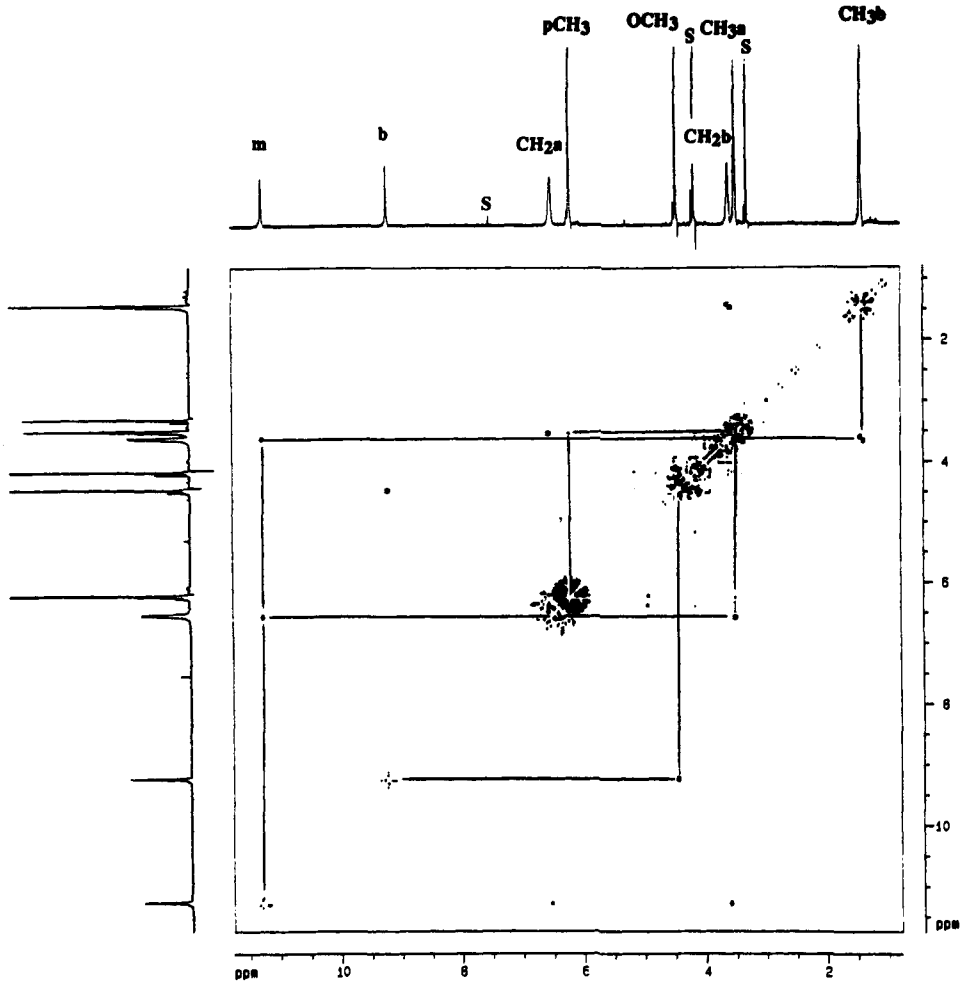

Figure 4. ROESY (323 K) spectrum of the Nd(III) texaphyrin complex **NdTx(NO$_3$)$_2$** (8 mM solution in CDCl$_3$/CD$_3$OD 2:1 v/v, 296 K). One peak (that of the imino hydrogen) lies outside the observed spectral region. S denotes signals arising from the solvent and DHO.

Table 2. Fitting Results for the Nitrate Derivatives of Lanthanide Texaphyrins **LnTx(NO$_3$)$_2$** (D_1, D_2, α, Agreement Factors R, and Calculated Contact Shift Values for the Imino Protons δ_{conI}[i] for a Model Excluding the Imino Positions from the Initial Calculations. Also Shown Are Agreement Factors R' for Fits Carried Out Using a Model That Includes All Positions (See Text for Details)

	Ce	Pr	Nd	Eu	Tb	Dy	Ho	Er	Tm	Yb
D_1[a]	209	493	363	−364	8024	11588	7036	−3039	−6005	−4196
D_2[a]	−214	−696	−597	557	−6489	−13360	−7523	1159	3398	1931
α[b]	−16.2	−29.7	−19.9	−22.6	−19.1	−19.1	−21.6	−4.8	−17.2	−19.2
R	0.195	0.125	0.168	0.259	0.084	0.096	0.075	0.114	0.072	0.066
R'	0.282	0.282	0.362	0.421	0.274	0.212	0.212	0.258	0.076	0.053
δ_{conI}[i,c]	3.50	9.61	13.14	−25.9	−74.39	−66.88	−41.04	−35.73	−13.09	−4.18

[a] (ppm × Å). [b] (deg). [c] (ppm).

experimental data could be fit using but two parameters. As expected, the fits were rather poor. Indeed, agreement factors R (see eq 1) ranging from 21.1% for the Yb(III) system **YbTx(NO$_3$)$_2$** to 44.2% for the trivalent Eu texaphyrin **EuTx(NO$_3$)$_2$** were observed. Much better fits were obtained when a more general rhombic susceptibility tensor ($D_1 \neq 0$, $D_2 \neq 0$) was assumed; under conditions of this kind of three-parameter fit, R was found to range from 5.3% (for **YbTx(NO$_3$)$_2$**) to 42.1% (for **EuTx(NO$_3$)$_2$**); cf. Table 2.

The theoretical values for the ratio of the contact to dipolar contributions to the isotropic shift should be on the order of 0.06:0.1:0.4:1:−1.4:−0.11:−0.22:0.17:0.06:0.04 (normalized to 1 for Eu(III)) for an isostructural series of trivalent Ce, Pr, Nd, Eu, Tb, Dy, Ho, Er, Tm, and Yb lanthanide complexes.[22,25] Thus, good fits, according to the dipolar model, are expected in those cases (i.e., Yb(III) and Tm(III)) where the lowest theoretical contact contribution is predicted. On the other hand, less acceptable fits would be expected in those cases (i.e., Eu(III) and Nd(III)) where relatively important contact shift effects are predicted. As illustrated by the data in Table 2, this indeed proved to be the case. Thus, contact shifts, although generally not dominant, may not be completely ignored.

Since we did not want to include new parameters (i.e., contact shifts) into our fitting procedures (even though, of course, adding new parameters would make the R values smaller), we tried to factor out all contact contributions. This was done by selecting in an iterative fashion those data points (i.e., positions) that were to be explicitly excluded from our fitting calculations. The relevant shifts for these latter were then not included in the calculation of R factors, since doing so would be equivalent to adding a new fitting parameter (see below).

While many such "gedanken" experiments were carried out for various single positions, the dramatic improvements in the

(25) Golding, R. M.; Halton, M. P. *Aust. J. Chem.* **1972**, *25*, 2577.

Table 3. Comparison of Measured Isotropic Shifts $\delta_{iso\ meas}$ and Calculated Dipolar Shifts $\delta_{dip\ cal}$ for the Yb(III) Texaphyrins. These Latter Were Derived Using a Model That Excludes the Imino Protons from the Fitting Procedure (See Text for Details)

proton	$\delta_{dip\ cal}$ (ppm)	D_1G_1 (ppm)	D_2G_2 (ppm)	$\delta_{iso\ meas}$ (ppm)
A. Dinitrate Complex **YbTx(NO$_3$)$_2$**. $D_1 = -4196.13$ (ppm × Å), $D_2 = 1931.39$ (ppm × Å), Rotation Angle $\alpha = -19.2°$, and $R = 6.60\%$				
1 imino	−51.65	−47.86	−3.79	−55.83
2 meso	−30.10	−32.23	2.13	−30.88
3 benzo	−19.91	−27.68	7.78	−19.72
4 CH_2a	−18.80	−13.71	−5.09	−19.60
5 *p*-CH_3	−22.82	−15.66	−7.16	−23.17
6 OCH_3	−4.55	−8.07	3.51	−4.98
7 CH_3a	−15.60	−11.50	−4.09	−13.17
8 CH_2b	−7.25	−12.98	5.73	−7.85
9 CH_3b	−6.35	−11.11	4.76	−4.55
B. Diphenyl Phosphate Complex **YbTx(P1)$_2$**. $D_1 = -11.98$ (ppm × Å), $D_2 = 3764.92$ (ppm × Å), Rotation Angle $\alpha = -14.9°$ and $R = 7.17\%$				
1 imino	−8.45	−0.13	−8.33	−13.75
2 meso	4.80	0.10	4.90	5.37
3 benzo	14.49	−0.07	14.57	14.99
4 CH_2a	−9.80	−0.04	−9.76	−9.68
5 *p*-CH_3	−14.10	−0.04	−14.05	−15.27
6 OCH_3	6.67	−0.02	6.69	5.74
7 CH_3a	−7.87	−0.03	−7.84	−7.19
8 CH_2b	11.55	−0.04	11.59	11.23
9 CH_3b	9.59	−0.04	9.63	8.56
C. Phenylphosphonate Complex **YbTx(P2)$_2$**. $D_1 = 1989.17$ (ppm × Å), $D_2 = 3973.11$ (ppm × Å), Rotation Angle $= -17.6°$, and $R = 6.98\%$				
1 imino	14.05	22.18	−8.13	8.21
2 meso	20.44	15.74	4.69	21.43
3 benzo	28.62	12.82	15.80	28.89
4 CH_2a	−3.81	6.60	−10.41	−3.23
5 *p*-CH_3	−7.40	7.37	−14.77	−8.72
6 OCH_3	10.93	3.75	7.18	10.86
7 CH_3a	−2.83	5.54	−8.36	−2.89
8 CH_2b	18.38	6.42	11.96	18.63
9 CH_3b	15.43	5.49	9.94	12.85

relevant R factors were obtained only when the imino protons were excluded from the fitting procedure of eq 4.[26] Once good fits were obtained in this way, the calculated parameters (D_1, D_2, and α) could be used, in turn, to calculate the dipolar shifts for the omitted imino protons (cf. Table 3). Subsequently, the contact shifts were obtained by subtracting the calculated dipolar contributions from the measured isotropic shifts. The resulting values, which were found to be substantial, are presented in Table 2.

The same magnetic anisotropy parameters and contact shifts for the non-imino protons were derived when the contact shifts of the imino proton were used as fitting parameters. Now the R values (eq 1) were found to range from 4.4% for the Yb(III) complex to 8.0% for the Tb(III) one. Although gratifying, this internal consistency is not surprising. This is because, for any set of magnetic anisotropy parameters, contact shift values equal to $\delta^{obs}{}_{iso} - \delta^{calc}{}_{dip}$ can be found such that $\delta^{obs}{}_{iso} - \delta^{calc}{}_{dip+cont} = 0$ in every position for which the contact shift was used as a fitting parameter. Hence the minimum of the numerator in eq 1 can be found as follows:

$$\min\left(\sum_{i=1}^{n}(\delta_i^{obs} - \delta_i^{calc})^2\right) = 0 + \min\left(\sum_{i=k+1}^{n}(\delta_i^{obs} - \delta_i^{calc})^2\right) \quad (4)$$

where for n observed shifts, the contact shifts for the 1, 2, ... k positions are used as the fitting parameters. Thus, finding the minimum R value in a procedure, including contact shifts for the first k positions, is equivalent to finding the minimum of R in a procedure omitting these positions from a calculation of dipolar shifts (identical values are obtained in the numerator term of eq 1). In other words, a procedure including contact shifts for a given set of positions as unconstrained fitting parameters will produce the same contact shift and magnetic susceptibility tensor values as a fitting procedure omitting these positions.

In our case, these two methods correspond to $n \times (3 + k)$ and $(n - k) \times 3$ fits, and, in the general case, correspond to $n \times (5 + k)$ and $(n - k) \times 5$ fits. (Here n is the number of observed shifts and k is the number of positions for which contact shifts are considered. The values to the left of the symbol × denote the number of resonances included in calculations and those to the right denote the number of fitting parameters.) There is, of course, a difference in the numerical values of R obtained using these two types of fitting procedures. This is simply a reflection of the fact that, although the numerator terms in these two expressions for R will be the same, the denominator in the first case will contain more elements.

In cases where the omitted positions show exceptionally large experimental shifts, the above differences in calculated R values can be very large; for instance, for the Eu(III) texaphyrin complex **EuTx(NO$_3$)$_2$**, the R value is calculated to be 25.9% when using the 8 × 3 fit but only 4.5% when using the 9 × 4 fitting procedure (in this case, $n = 9$, $k = 1$). However, it is critical to appreciate that obtaining low values of R by using a higher number of fitting parameters does not necessarily mean that the fit is better. Indeed, in our opinion, the low values of R that can be obtained in, e.g., an $n \times (5 + k)$ fit are misleading; looking for relative improvements in R value using an $(n - k) \times 5$ procedure is a much more effective way to gauge whether it is appropriate or necessary to consider introducing contact shifts into the modeling procedure.

When this same "selective fitting" procedure is applied to the same series of nitrate complexes (i.e., those of general type **LnTx(NO$_3$)$_2$**), but now omitting not just the imino but the meso and benzo protons as well, the "extra" improvements in the values for R (ranging from 17.3% for the Eu(III) to 6.9% for the Ho(III) texaphyrin complexes, respectively) are not dramatic.[27] In fact, even for those complexes with relatively large contact shifts, the contact shifts calculated for the meso and benzo protons were generally found to be an order of magnitude smaller than those of the imino proton. Furthermore, they were found to be comparable to the difference between δ_{iso} measured and δ_{dip} calculated for the "remaining" protons (i.e., those included in the fit). Likewise, the specific values of the contact shifts for the imino positions calculated using this process are similar to those obtained when only the imino shifts were omitted. Finally, the derived contact shifts for the meso and benzo positions were found to be inconsistent with the theoretical $\langle S_z \rangle$ values (see below). It thus follows that the contact shifts for these non-imino protons cannot be reliably found by this procedure. Nonetheless, it is clear that any contact shift contributions to the observed meso-H and benzo-H signals, due to π delocalization or other effects, are necessarily rather small.

Interestingly, this method of analyzing contact contributions proved to be superior to other methods described in the literature (see supplementary material for comparison).

(26) The one exception is the Yb(III) complex **YbTx(NO$_3$)$_2$** for which the R factor increases slightly but remains nonetheless very good. In this instance, the small increase in R could simply reflect the exclusion of the large $(\delta^{obs}{}_{iso})^2$ (imino) term from the denominator of the expression for R.

(27) The same values of D_1, D_2, α, and of the contact shifts for the imino, meso, and benzo protons were obtained when the last three were introduced as fitting parameters. In these cases, the R value ranged from 6.7% for **DyTx(NO$_3$)$_2$** to 2.9% for **EuTx(NO$_3$)$_2$**.

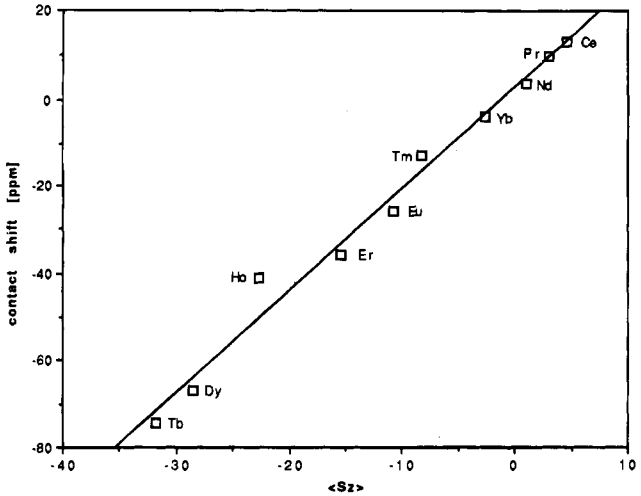

Figure 5. Plot of calculated contact shifts of imino proton vs theoretical $\langle S_z \rangle$ values. See text for details.

(2) Discussion of Calculated Contact Shifts and Magnetic Anisotropy. The analysis of contact shifts in terms of theoretical values alluded to above was made using eq 5.[25]

$$\delta_{cont} = A'\langle S_z \rangle = A\langle S_z \rangle / \gamma\hbar B_0 \qquad (5)$$

According to this equation, the contact shifts of a given position should be proportional to the $\langle S_z \rangle$ value of the lanthanide ion in question, assuming the same hyperfine constants A_i hold throughout the entire Ln(III) texaphyrin series. In point of fact, plots of contact shifts for the imino protons (derived from $(n - 1) \times 3$ fits (i.e., one position omitted) as described above) vs theoretical $\langle S_z \rangle$ values gave a surprisingly good correlation (Figure 5).[28] The quality of the plot is astonishing when one considers the indirect method used to evaluate the contact shifts. It is thus tempting to consider the quality of this correlation as a vindication not only of the calculational procedure as a whole but also of the various magnetic parameters (dipolar shifts) from which the contact shifts were originally derived.

An assessment of magnetic anisotropy effects is another portion of the general analysis that is important for a full characterization of the system. In the case of the lanthanide nitrate complexes **LnTx(NO$_3$)$_2$**, the calculated α values (Table 2) indicate that the magnetic z axis is nearly perpendicular to the macrocyclic plane, in accord with intuition. (An α value of $-16.0°$ would correspond to the z axis being perpendicular to the macrocycle plane in the X-ray structure of **GdTx(NO$_3$)$_2$**). The χ tensors, however, are highly rhombic. Thus, the axial and rhombic contributions to the dipolar shifts, given by the first and second terms, respectively, of eq 3, are comparable in absolute magnitude, albeit of opposite sign, for many positions. Examples of these contributions are presented in Table 3 and in the supplementary material.

None of the principal χ values is particularly unique; that is, $|\chi_z - \chi_x|$ is similar to $|\chi_x - \chi_y|$. In fact, the latter term is slightly bigger for the trivalent Ce, Pr, Nd, Eu, Dy, and Ho complexes. This means that the y axis as defined in Figure 1 could equally well be chosen as being the unique (i.e., z) axis. For such a choice, the magnetic x and y axes (corresponding to the former x and z axes) would need to be rotated around the new z axis in the fitting procedures. Once this is done, however, the various calculation-derived results of interest (i.e., dipolar shifts, α, and R values as well as $\chi_z - \chi_x$ and $\chi_x - \chi_y$ corresponding to the $\chi_y - \chi_x$ and $\chi_x - \chi_z$ terms of the original axis labeling choice) would, of course, end up being the same. The values of D_1 and D_2, however, would end up being different; these are presented in the supplementary material.

On first sight it is surprising that plots of dipolar shift vs theoretical C_j coefficients are of worse quality then are plots of the contact contribution vs the $\langle S_z \rangle$ coefficients. In addition, plots of the parameters D_1 and D_2 vs the coefficients C_j show large deviations from linearity (cf. supplementary material). However, on the basis of eq 3 and Bleaney's equation[22] (eq 6, wherein $\langle r^k \rangle A_k^q$ represent the crystal field coefficients, k is Boltzmann constant, T is temperature, and the other symbols have the same meaning as in eq 3), D_1 and D_2 should be proportional to the coefficients C_j.

$$\delta_{dip} = C_j[\mu_B^2\langle r^2 \rangle 2A_2^0(3\cos^2\theta - 1) + \mu_B^2\langle r^3 \rangle 2A_2^2 \sin^2\theta \cos 2\varphi]/60(kT)^2 r^3 \qquad (6)$$

In fact, the deviations of D_1 and D_2 are of opposite sign and are strikingly proportional. This suggests that the deviations observed in the plots of D_1 and D_2 vs C_j are not mainly due to errors in the derived D values, but to other reasons, such as, e.g., non-isostructurality within the series of nitrate complexes **LnTx(NO$_3$)$_2$** or inadequacies in the relevant C_j parameters.

The ratio of D_1 to D_2 is -0.98, -0.71, -0.61, -0.65, -1.27, -0.87, and -0.94 respectively for the Ce(III), Pr(III), Nd(III), Eu(III), Tb(III), Dy(III), and Ho(III) series of dinitrate texaphyrin complexes and -2.62, -1.77, and -2.17 for the corresponding trivalent Er, Tm, and Yb adducts, respectively. For the Er(III), Tm(III), and Yb(III) texaphyrin dinitrate complexes, defining the z axis as being roughly perpendicular to the macrocycle plane indeed provides a unique choice for the magnetic axes ($|\chi_z - \chi_x| \gg |\chi_x - \chi_y|$); this is as expected for these "more axial" complexes. According to eqs 3 and 6 the change in this ratio corresponds to a change in the ratio of the crystal field parameters $\langle r^k \rangle A_k^q$ and thus could reflect an abrupt change in the structure of the lanthanide texaphyrin nitrate complexes between Ho(III) and Er(III).

As is discussed in considerable detail elsewhere,[2,10] slight but significant variations in both total coordination number and local geometry are apparent when the series of crystallographically characterized Ln(III) texaphyrin nitrate complexes are considered *in toto*. In the case of the structurally characterized La(III) texaphyrin nitrate complex **LaTx(NO$_3$)$_2$**,[2,10] for instance, the metal cation ion was found to be ca. 0.91 Å out of plane in the solid state and 10-coordinate with two bidentate nitrates and one methanol molecule acting as the axial ligands. In the corresponding isostructural Eu(III) and Gd(III) complexes, **EuTx1(NO$_3$)$_2$** and **GdTx1(NO$_3$)$_2$**,[2,10] the metal center is ca. 0.60 Å out of the plane and 9-coordinate with, in this case, one bidentate nitrate and two methanol axial ligands serving as the apical ligands. By contrast, the near-analogous Tb(III) complex **TbTx1(NO$_3$)$_2$**[2] displays fully in-plane 9-coordination, while the Gd(III) complex **GdTx(NO$_3$)$_2$** demonstrates both out-of-plane 9- and out-of-plane 10-coordination in the solid state.[2,10] Finally, the 8-coordinate diamagnetic Lu(III) **LuTx2(NO$_3$)$_2$** complex displays near in-plane coordination of the metal center in spite of an unsymmetric "top face" bidentate nitrate and "bottom face" monodentate methanol axial ligand coordination environment.[2,10] Thus, the invoked changes in the crystal field parameters, $\langle r^k \rangle A_k^q$ could correspond to, e.g., changes from what are predominantly 9-coordinate species for Ho(III) to predominant 8-coor-

(28) Similar plots, using values of the imino contact shifts derived from the $(n - 3) \times 3$ fitting procedure, show larger deviations from linearity, and the correlation of the meso and benzo positions with $\langle S_z \rangle$ values is very poor. Thus this analysis supports the conclusion that the smaller R values obtained using a $(n - 3) \times 3$ fit are not very meaningful and the imino protons need only be analyzed in terms of appreciable contact shifts.

Scheme 2. Simplified Axial Ligand Exchange Equilibria for Lanthanide Texaphyrins (Coordinated Solvent Omitted)

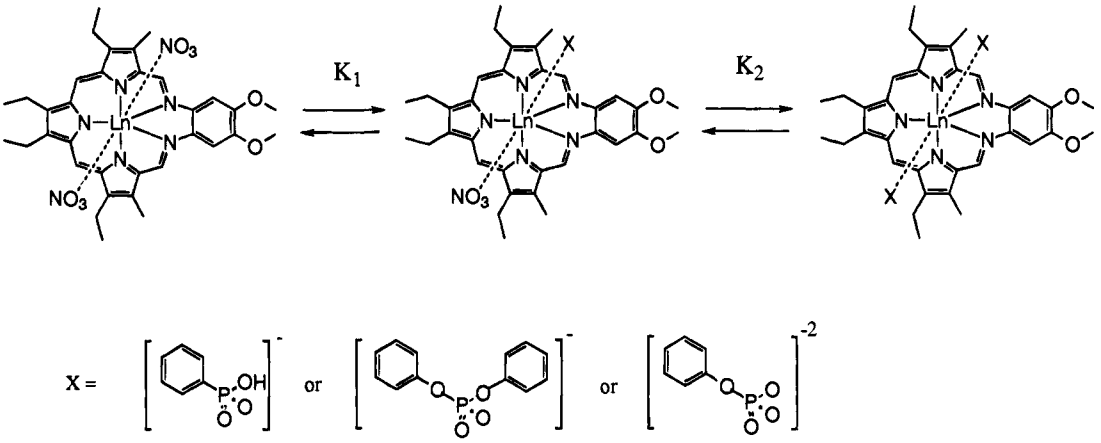

Table 4. Isotropic Shifts (ppm) of Lanthanide(III) Texaphyrin Diphenyl Phosphate (**LnTx(P1)$_2$**) and Phenylphosphonate (**LnTx(P2)$_2$**) Complexes

	TbP1	DyP2	DyP1	HoP1	ErP1	TmP2	TmP1	YbP2	YbP1
imino	5.55	−157.40	−43.03	14.27	−19.55	−18.25	−45.48	8.21	−13.75
meso	−32.57	−139.60	−40.15	7.36	11.16	17.99		21.43	5.37
benzo	−49.22	−55.00	−85.71	−26.24	13.93	33.65	15.21	28.89	14.99
CH_2a	19.14	−90.00	34.21	35.30	−1.98	−13.81	−21.21	−3.23	−9.68
p-CH_3	24.10	−66.50	51.18	47.37	−4.87	−22.66	−30.19	−8.72	−15.27
OCH_3	−11.99	−15.30	−30.68	−11.68	4.50	12.17	6.55	10.86	5.74
CH_3a	11.91	−45.90	23.95	24.21	−1.45	−9.61	−14.51	−2.89	−7.19
CH_2b	−22.63	−11.50	−59.78	−25.01	7.46	22.79	13.05	18.63	11.23
CH_3b	−18.05	−17.50	−44.12	−21.24	5.99	18.08	11.23	12.85	8.56

dinate ones for Er(III), Tm(III), and Yb(III) texaphyrins *in solution*. Likewise, a change in coordination number/geometry (from, presumably, out-of-plane 10-coordinate to out-of-plane 9-coordinate or in-plane 9-coordinate) is also possible between the Eu(III) and Tb(III) texaphyrin nitrate complexes **EuTx(NO$_3$)$_2$** and **TbTx(NO$_3$)$_2$**. To the extent that these abrupt changes in coordination number and geometry occur in solution, they would be expected to have a more substantial effect on the magnetic anisotropy parameters than on the hyperfine constants A_i. This lower sensitivity, in turn, would explain why, throughout the lanthanide series, a better correlation is found with theoretical parameters when contact shifts, as opposed to the dipolar shifts, are used.

Axial Ligation. The ^{1}H NMR spectra of the starting lanthanide texaphyrin nitrate complexes (studied as their well-characterized methanol adducts) are solvent dependent. This, presumably, reflects changes that arise as the result of solvent coordination. Although not a focus of the present paper, it is of interest to note that the spectra of these water soluble texaphyrin complexes, **LnTx1(NO$_3$)$_2$**, in water are generally similar to those of the methoxy series in methanol/chloroform. For instance, analogous positions (i.e., protons) have similar isotropic shifts. However, the signals are much broader. This could be due to a dynamic equilibrium involving one or more coordinated water molecules. To the extent that such thinking is correct, it is necessary to assume that the relevant interconversion rates are somewhat smaller than those for the corresponding methanol adducts; this slower exchange would then be the origin of the additional line broadening. It should be noted that an analysis of the exchange dynamics of coordinated water molecules is of critical importance to an interpretation of the relaxivity properties of, e.g., gadolinium(III) texaphyrins and to an assessment of the possible utility of this kind of complex in magnetic resonance imaging (MRI) applications. Thus, further analyses of the lanthanide(III) texaphyrins in aqueous media are currently ongoing. In the case of DMSO, the solvent appears to replace completely any methanol molecules originally present as evidenced by spectra that are distinct from, but not all that different than, those of the starting methanol adducts. By contrast, very broad signals are observed for various solutions of **LnTx(NO$_3$)$_2$** in pyridine-d_5. This suggests the presence of a more equal equilibrium between species containing pyridine and methanol in their metal-centered coordination spheres.

Turning to the question of anionic axial ligation, there are two main issues of interest that come to the fore. First, what is the extent to which "nitrate off" equilibria (cf. Scheme 1) contribute to definition of the species present in solution, and second, what are the kinetics and thermodynamics of various anion exchange processes such as those represented by Scheme 2?

Adding more than 10 molar equiv of $LiNO_3$ to methanolic solutions of the various lanthanide texaphyrin−nitrate complexes of general structure **LnTx(NO$_3$)$_2$** effect but little change in the corresponding paramagnetic ^{1}H NMR spectra (in all cases a less than 10% increase in the absolute isotropic shift is seen). These observations lead us to suggest that the equilibria associated with nitrate binding lie far toward the side associated with dinitrate adducts formation (i.e., toward structures such as **I** or **III** in Scheme 1). They thus serve to confirm the initial impressions of solution phase structure made on the basis of symmetry (vide supra).

In contrast to what is seen with nitrate, the addition of phosphate-type species (*viz.* diphenyl phosphate monoanion (**P1**$^-$), phenylphosphonate monoanion (**P2**$^-$), or phenyl phosphate dianion (**P3**$^{2-}$)) engenders a dramatic effect.[29] Not only are large changes in isotropic shift values observed but also, in the case of complexes with large dipolar shifts, completely new spectral patterns are actually observed (Figures 2 and 3, Table 4). Small differences in chemical shifts (compared to those of the paramagnetic species) are also seen when phosphate-for-nitrate exchange is effected in the case of the diamagnetic **LaTx(NO$_3$)$_2$** and **LuTx(NO$_3$)$_2$** complexes. Unfortunately, in the case

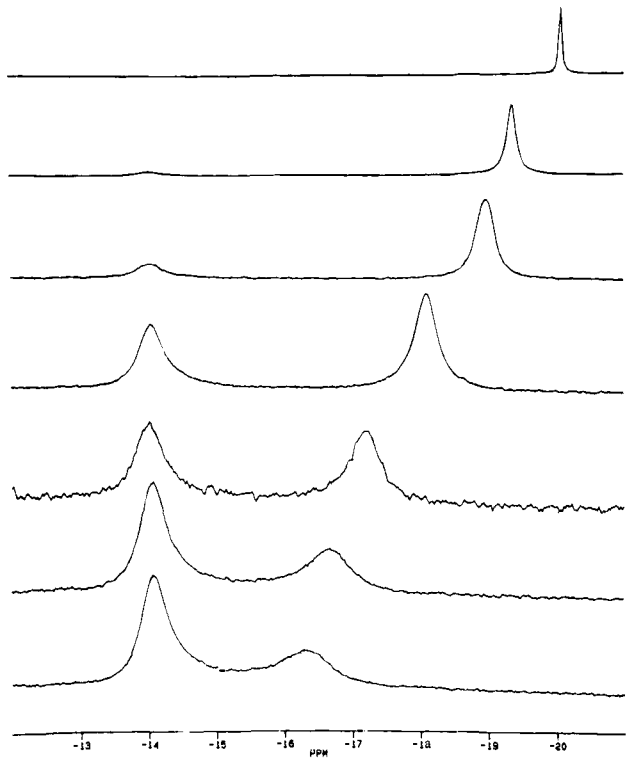

Figure 6. Proton NMR spectra of a 6.75×10^{-3} mM solution of Eu texaphyrin **EuTx(NO$_3$)$_2$** in $CD_3OD/CDCl_3$ (10:1 v/v) in the presence of (from top to bottom) 0, 0.45, 0.79, 1.45, 2.31, 3.47 and 4.34 molar equiv of sodium diphenyl phosphate.

of many of the paramagnetic species, not all of the texaphyrin signals are well-resolved. This, presumably, is the result of incomplete exchange in conjunction with unfavorable exchange rates. For the same reasons, the positions of the resonances associated with the phenyl rings of the phosphate-type ligands could not be determined in most cases.

Since the exchange of nitrate for other anions, notably phosphate-type ones, is not very fast on the NMR time scale and the lines are considerably broadened, it is very difficult (and in most cases, impossible) to follow the spectral changes in a titration-like fashion (i.e., as increasing aliquots of the "replacement anion" are added to the starting nitrate complexes).[30] Such titrations could not, therefore, be used to obtain binding constants directly. Nor, unfortunately, could they be generally used to make spectral assignments. One of the few exceptions to this former limitation came in the case of the Eu(III) system **EuTx(NO$_3$)$_2$**. Here, as illustrated by Figure 6, monotonic shifts in the imino proton signals are observed as sodium diphenyl phosphate is added to $CDCl_3/CD_3OD$ solutions of the starting dinitrate complex. In this case, interestingly, at least two processes are visible in the course of the titration. The first of these, corresponding to the initial exchange reaction

(29) Preliminary ligand exchange experiments using fluoride, chloride, acetate, and benzoate were also carried out with various **LnTx(NO$_3$)$_2$** complexes. As expected, it was found that anionic axial ligand exchange (where occurring) gives rise to discernible changes in the observed spectral pattern. Preliminary attempts were also made to study the interactions of simple phosphate anions (e.g., HPO_4^{2-} and $H_2PO_4^-$) with water-soluble lanthanide(III) texaphyrins of general structure **LnTx1(NO$_3$)$_2$**. Unfortunately, the species obtained were for the most part almost completely insoluble, possibly as the result of metal-to-metal polymerization mediated via bridging phosphate ligands.

(30) For the same reason, extrapolations of the chemical shift values for the phosphate derivatives out to infinite free axial ligand concentration were not made: at low phosphate concentrations the lines were too broad to follow, while at high phosphate concentration measurements were precluded by solubility problems.

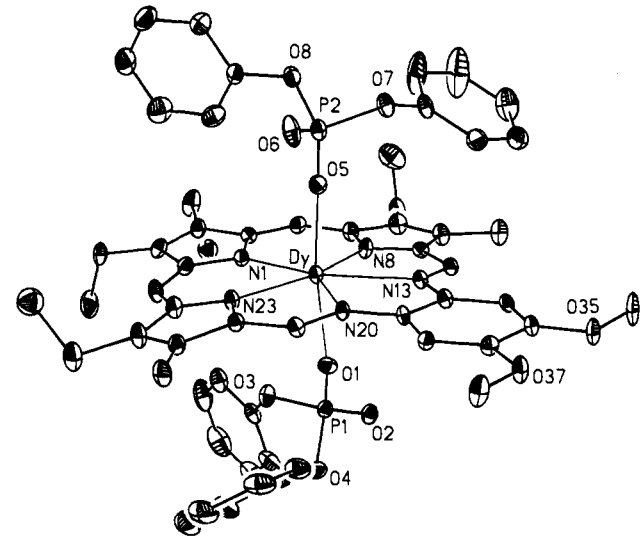

Figure 7. View of the Dy(III) texaphyrin complex in **DyTx(P1)$_2$**. The hydrogen atoms have been omitted for clarity. The thermal ellipsoids are scaled to the 30% probability level. The Dy(III) ion is 0.073 Å from the mean plane through the five nitrogen atoms of the macrocycle. Pertinent bond lengths (Å) and angles (deg): Dy–N1 2.437(4), Dy–N8 2.335(5), Dy–N13 2.438(4), Dy–N20 2.459(4), Dy–N23 2.317(5), Dy–O1 2.234(6), Dy–O5 2.222(6); O1–Dy–O5 169.2(1), N1–D6–N8 78.2(2), N1–Dy–N23 77.8(2), N8–Dy–N13 68.2(2), N13–Dy–N20 66.8(2), N20–Dy–N23 68.8(2).

of Scheme 2, is fast on the NMR time scale and gives rise to the time-averaged signal in the −20 to −16.5 ppm range. By contrast, the second process, corresponding to the formation of the bis(diphenyl phosphate) adduct, is slow on the NMR time scale. It results, therefore, in a steady increase in integrated spectral intensity for the signal at ca. −14 ppm.

The above spectral changes can be reversed by the addition of lithium nitrate. This particular finding supports the conclusion that this monoanionic phosphate ligand replaces the nitrate counteranions in the lanthanide coordination sphere, and not just the more-loosely-bound methanol molecules. Ascribing the two spectrally distinct processes of Figure 6 to counteranion exchange thus appears appropriate. To the extent this is true, the relevant equilibrium (i.e., exchange) constants K_1 and K_2, of Scheme 3 may be calculated as being 0.9 and 3.5, respectively. While not necessarily large, these are of sufficient magnitude that processes involving phosphate-for-nitrate replacement have to be considered (at least for this metal) as being potentially important *in vivo*.

The fact that two diphenyl phosphate ligands can coordinate to the metal center of a lanthanide texaphyrin complex was confirmed by X-ray crystallographic analysis of **DyTx(P1)$_2$** (Figure 7). Here the metal ion is 7-coordinate as it is in the case of some Cd(II) texaphyrins.[7b] The X-ray structure of **DyTx(P1)$_2$** resembles that of **TbTx1(NO$_3$)$_2$**,[2] except that in the former the coordinated anions are monodentate. Furthermore, as is true for **LuTx2(NO$_3$)$_2$**[10] and **TbTx1(NO$_3$)$_2$**, the out-of-plane displacement of the metal ion is small; the Dy(III) ion is only 0.073 Å from the mean plane through the five nitrogen atoms.

Pure crystalline samples of **DyTx(P1)$_2$** were also studied by ^{1}H NMR spectroscopy in solution. Here it was found that when **DyTx(P1)$_2$** was dissolved in $CDCl_3/CD_3OD$, spectra were obtained with signals that were somewhat broadened and shifted compared to those obtained when **DyTx(NO$_3$)$_2$** was treated with an excess of **P1**$^-$ in these same solvents. However, the original line widths and chemical shifts were reproduced once free diphenyl phosphate was added to solutions made up from

Table 5. Fitting Results for the Diphenyl Phosphate (**LnTx(P1)$_2$**) and Phenylphosphonate (**LnTx(P2)$_2$**) Derivatives of Texaphyrins (D_1, D_2, α), Agreement Factors R, and Calculated Contact Shift Values for the Imino Protons $\delta_{con}{}^{i}$ for a Model Excluding the Imino Positions from the Initial Calculations (See Text for Details)

	TbP1	DyP2	DyP1	HoP1	ErP1	TmP2	TmP1	YbP2	YbP1
$D_1{}^{a,d}$	−2171	−15305	−2856	2304	931	1069	−1514	1989	−12
$D_2{}^{a,d}$	−7859	7724	−16244	−10286	1898	6617	6128	3973	3765
$\alpha^{b,d}$	−20.7	−9.6	−19.0	−14.7	−17.3	−16.5	−14.4	−17.6	−14.9
R^d	0.211	0.207	0.051	0.069	0.133	0.065	0.079	0.070	0.072
$\delta_{con}{}^{i\,c,d}$	16.05	8.24	−42.58	−33.09	−25.95	−15.96	−15.73	−5.84	−5.30
$D_1{}^{a,e}$	−2054		−2618	1815	776		−1343		−54
$D_2{}^{a,e}$	−7466		−15222	−9764	1791		5715		3512
$\alpha^{b,e}$	−12.1		−9.6	−20.3	3.9		−0.8		2.4
R^e	0.204		0.046	0.084	0.119		0.086		0.061
$\delta_{con}{}^{i\,c,e}$	11.52		−50.74	−39.87	−24.76		−10.94		−2.92

[a] (ppm × Å). [b] (deg). [c] (ppm). [d] Based on **GdTx(NO$_3$)$_2$** structure. [e] Based on **DyTx(P1)$_2$** structure; in this case an α value equal to −1.7° would place the z axis perpendicular to the macrocyclic plane.

crystalline **DyTx(P1)$_2$**. This clearly demonstrates that for **DyTx(P1)$_2$** partial dissociation of one of the axial phosphate-type ligands takes place in solution.

In the case of **CeTx(P1)$_2$**, **PrTx(P1)$_2$**, **NdTx(P1)$_2$**, and **EuTx(P1)$_2$**, where the dipolar shifts are relatively small, some resonances can be assigned by making appropriate comparisons back to the "parent" bisnitrate complexes. In the case of the **TbTx(P1)$_2$**, **DyTx(P1)$_2$**, **HoTx(P1)$_2$**, **ErTx(P1)$_2$**, **TmTx(P1)$_2$**, and **YbTx(P1)$_2$** complexes, resolved signals were observed (Figures 2 and 3, Table 4). Partial peak assignments could therefore be made on the basis of integration and line width analyses. These assignments were completed and verified by checking the goodness of fit to the dipolar model, as was done for the original dinitrate derivatives. Moderate R values (Table 5) were found for the **TbTx(P1)$_2$** and **ErTx(P1)$_2$** complexes, but good fits were obtained for the Dy(III), Ho(III), Tm(III), and Yb(III) systems.

The fitting results show (Table 5) that the D_1 and D_2 change completely in comparison to those of the starting dinitrate complexes. Now, the absolute value of D_2 is larger than D_1 and the second "rhombic" term of eq 4 dominates the first "axial" one (cf. Table 3). In the case of **TbTx(P1)$_2$**, **DyTx(P1)$_2$**, **ErTx(P1)$_2$**, and **TmTx(P1)$_2$**, the x axis is correlated with a unique χ value (i.e., $|\chi_x - \chi_y| > |\chi_y - \chi_z|$), so the changes in the magnetic anisotropy parameters may be equivalently described in terms of a rotation of the unique magnetic direction from off the perpendicular (original z direction) and into the macrocyclic plane (original x direction). In other words, the rotation angle relative to the starting axes system can be designated as being $\alpha' = \alpha + 90°$ instead of α; this corresponds to a rotation of the z axis toward the original x direction (cf. supplementary material for examples of calculations supporting this choice of α values).

The above results are not totally without precedent. For instance, similar, axial ligand correlated changes in the direction of the principal magnetic axis (i.e., from normal to the macrocycle plane to within the plane) have been previously observed by EPR spectroscopy in the case of copper(II)[31] and Ni(I)[32] macrocyclic complexes. A somewhat similar situation was also observed for a series of substituted low-spin iron(III) porphyrins,[33] wherein the into-macrocycle-plane switch of the principal magnetic axis results from changes in the substitution pattern about the periphery of the porphyrin ring.

Addition of monosodium phenyl phosphate to various initially pure solutions of **LnTx(NO$_3$)$_2$** also brings about complete changes in the spectral patterns. Unfortunately, however, in no case could a full assignment of signals be made. On the other hand, with phenylphosphonate, it proved possible to assign the ^{1}H NMR resonances in the case of the **DyTx(P2)$_2$**, **TmTx(P2)$_2$**, and **YbTx(P2)$_2$** complexes (Table 4, Figure 2, and supplementary Figure 8). Here, the observed isotropic shifts fit well, with the exception of the Dy(III) complex, to the theoretical model (Table 5). However, as above, x was found to be the unique magnetic axis.

While initially puzzling, the changes in the magnetic anisotropy parameters can be interpreted with the aid of eq 6. From this equation, it is apparent that changes in the value of D_1 and D_2 actually reflect changes in the relevant crystal field parameters $\langle r^k \rangle A_k^q$. Since the relative D_1 and D_2 values in the phosphate-type complexes are completely different from those of either the Ce(III)−Ho(III) or Er(III)−Yb(III) series of starting dinitrate complexes (when D values for the same original axis system are compared), it may safely be inferred that the changes in magnetic anisotropy observed between nitrate and phosphate series do not reflect only possible changes in the overall coordination number. Rather, they reflect, more probably, possible fundamental differences in the strengths of the relevant anion-to-lanthanide cation interactions. It is of interest to note that, for a given metal center, the contact shifts calculated for the imino protons are, for the most part, similar in both the nitrate and phosphate series (Tables 2 and 5).[34]

Substantial effects on the observed chemical shifts due to changes in axial ligands (provided by solvent or counteranions) have been reported previously in the case of paramagnetic lanthanide(III) complexes derived from hexaazamacrocycles.[35] In this instance, the authors ascribed these effects to the influence of the axial ligands on the conformation of the macrocycle. On the other hand, our study shows that those effects can arise mainly from changes in magnetic anisotropy brought about as the result of changes in the relevant crystal field (i.e., without having to invoke extreme changes in macrocyclic geometry or equatorial ligand binding modes).

At present, we are hoping to use the profound spectral changes accompanying the binding of phosphate-type ligands as a means whereby the interactions of lanthanide(III) texaphy-

(31) (a) Attanasio, D.; Collamati, L.; Cervone, E. *Inorg. Chem.* **1983**, *22*, 3281. Agostinelli, E.; Attanasio, D.; Collamati, I.; Fares, V. *Inorg. Chem.* **1984**, *23*, 1162.

(32) Chmeielewski, P.; Grzeszczuk, M.; Latos-Grazynski, L.; Lisowski, J. *Inorg. Chem.* **1989**, *28*, 3546.

(33) Isaac, M. F.; Lin, Q.; Simonis, U.; Suffian, D. J.; Wilson, D. L.; Walker, F. A. *Inorg. Chem.* **1993**, *32*, 4030.

(34) The difference in contact shift values observed for the Tb(III) diphenyl phosphate and Dy(III) phenylphosphonate texaphyrin complexes as compared to those of the "starting" nitrate adducts is probably due to large errors inherent in the calculations (large R values; cf., Table 5) rather than to some specifically important chemical effect. In both cases, the signals are considerably broadened, leading us to suggest that the relevant ligand metathesis process is far from complete.

(35) Benetollo, F.; Polo, A.; Bombieri, G.; Fonda, K. K.; Vallarino, L. M. *Polyhedron* **1990**, *9*, 1411.

rins with biomolecules, in particular oligonucleotides, may be probed. In this context, preliminary results, involving the use of simple nucleotides in methanol and degraded DNA (i.e., a deoxyoligonucleotide mixture) in water, are considered promising; they confirm that substantial changes in the paramagnetic ^{1}H NMR lanthanide(III) texaphyrin spectral patterns may be induced by these putative anionic ligands. This, in turn, suggests that the methods and results presented in this paper will be of use as more detailed insights into the mechanism of lanthanide(III) texaphyrin mediated RNA hydrolysis are sought.

Acknowledgment. Support for this work from the National Institutes of Health (AI 28845) and Pharmacyclics Inc. is gratefully acknowledged. We are grateful to Prof. A. Dean Sherry for having read through critically an early draft of this paper.

Supplementary Material Available: Discussion of alternative methods of estimating contact shifts, examples of fitting results for alternative axis systems, plot of D_1 and D_2 parameters vs C_j coefficients, plots of representative shifts of **LnTx(NO$_3$)$_2$** complexes vs C_j coefficients, temperature dependencies of representative signals of **NdTx(NO$_3$)$_2$** and **TbTx(NO$_3$)$_2$** complexes, ^{1}H NMR spectra of **EuTx(NO$_3$)$_2$**, **SmTx(NO$_3$)$_2$**, **CeTx(NO$_3$)$_2$**, **TmTx(NO$_3$)$_2$**, **TmTx(P1)$_2$**, and **TmTx(P2)$_2$**, COSY and NOE difference spectra of **NdTx(NO$_3$)$_2$**, detailed experimental data for X-ray diffraction, fractional atomic coordinates, anisotropic thermal parameters, bond lengths and angles, and atom labeling schemes for **DyTx(P1)$_2$** (41 pages); table of observed and calculated structure factors for **DyTx(P1)$_2$** (19 pages). This material is contained in many libraries on microfiche, immediately follows this article in the microfilm version of the journal, can be ordered from the ACS, and can be downloaded from the Internet; see any current masthead page for ordering information and Internet access instructions.

JA943191C